Modification effects of as cast Mg-Al-Si magnesium alloy with strontium

WANG BAOGANG[a], WANG XU[*,a,b], ZHOU JIXUE[b], LIU YUNTENG[b], LIANG PING [a], WANG YUNLING[a], ZHANG GUOFU[a]
[a]*School of Mechanical Engineering, Liaoning Shihua University, Fushun 113001, P. R. China*
[b]*Institute of New Materials, Shandong Academy of Sciences, Jinan 250013, P. R. China*

This paper reported modification effects of as cast AS31 magnesium alloy with strontium (Sr=0, 0.2, 0.4, 1 wt. pct). Strontium (Sr) was an effective grain-refiner in AS alloys. The results indicated that adding 0.2 wt. %, 0.4 wt. %Sr and 1.0 wt. %Sr to AS31 alloy, the Chinese script Mg_2Si phases were modified and refined obviously. The Mg_2Si phase changed from coarse Chinese shape to fine granule and irregular polygonal shapes. Sr could attach to the Mg_2Si peripheral, forcing primary Mg_2Si balling and suppressing dendritic structure and/ or twice dendrites orientation of dendrite Mg_2Si Chinese script phase. Sr was likely to combine with the Si to produce acicular Si_2Sr phase.

(Received September 6, 2013; January 22, 2014)

Keywords: Mg-Al-Si magnesium alloy, Modification, Strontium, Grain refine

1. Introduction

AS the lightest applied structural alloys, magnesium alloys offer many advantages such as low density, good combination of castability and mechanical properties. Recent research and development studies of magnesium alloys have been greatly promoted by the lightweight requirement in the automotive industry [1-4]. The Mg–Al–Si (AS) magnesium alloys offer good creep resistance and low cost which can meet the materials requirements for automotive powertrain applications [5-7]. In the AS alloys, the stable Mg_2Si phase exhibits high melting temperature, low density, high hardness and low thermal expansion coefficient. However, the Mg-Al-Si alloy shows low ductility and strength due to the coarse Chinese script Mg_2Si phase. Therefore, the modification and refinement of Mg_2Si phase is one of the means to improve the mechanical properties of Mg-Al-Si based alloys [8-9].

Previous experiments had shown that Si-containing magnesium alloy after Sr modification, relative to other alloy element, Sr microalloying had advantages of obvious effect, process simple and less addition, low cost. Generally, Zr addition was considered to be the most reliable and effective grain refiner for magnesium alloys, but couldn't be used for Mg–Al alloys as it reacts with aluminum [10]. Strontium (Sr) had effectively led to grain refinement of Mg-Al alloys. It was thought to be a potential alloying and/or microalloying element for Mg-Al based wrought and casting alloys [11-13], the morphology modification of the secondary phase Mg_2Si particles from Chinese script shape to refined polygonal shape was greatly affected by the addition of Sr [14].

In the present study, we selected Mg-3Al-1Si (wt. pct) as a base alloy composition and Sr as a quaternary element addition to explore the modification effects for the AS31 alloys.

2. Experimental procedures

AS31 magnesium alloys were prepared from pure Mg ingot (99.97 wt. %), Al ingot (99.95 wt. %), high purity Mg10wt. %Si and Mg–10wt. %Sr master alloys. The experimental alloys were melted in an electrical resistance furnace and protected by SF_6+CO_2 atmosphere. The pure Mg was first melted, Stirring and adding an appropriate amount of pure aluminum ingot when the temperature was raised to 680 ℃, then when the melt temperature reached approximately 720 ℃, the Mg–Si and Mg–Sr master alloys were added to the melt. After being homogenized by mechanical stirring and mixed completely, the melt was held at 750 ℃ for 30 min and then poured into a permanent mold which was preheated to 200 ℃. For comparison, the AS31 alloy without Sr addition was also cast under the same conditions as the above samples, and the microstructural analysis was also carried out under the same conditions. The chemical composition of the samples was determined with the inductively coupled plasma atomic emission spectroscopy (ICP-AES) method. The chemical compositions of the alloys are listed in Table 1.

Table 1. Actual compositions of the experimental alloys, wt. %.

Nominal alloys	Al	Si	Sr	Mn	Mg
AS31	3.25	0.92		0.38	Bal.
AS31+0.2Sr	3.24	0.91	0.21	0.39	Bal.
AS31+0.4Sr	3.11	1.21	0.38	0.33	Bal.
AS31+1.0Sr	3.40	1.16	1.06	0.41	Bal.

Data are given as wt. pct

The samples of the as-cast experimental alloys were examined by a TESCAN VEGA II LMU type scanning electron microscope (SEM), with secondary electron (SE) and backscattered electron (BSE) detectors, operated at 30 kV. The distributions of the different elements in the as-cast experimental alloys were analyzed using an Oxford energy dispersive spectrometer (EDS). The phases in the as-cast experimental alloys were also analyzed by a MAXima_X XRD-7000 X-ray diffractometer (XRD).

3. Results

The typical microstructure of AS31 is shown in Fig. 1(a), before the adoption of the XRD analysis combined with EDS analysis showed that, AS31 magnesium alloy mainly consisted of the matrix α-Mg, divorced eutectic β-$Mg_{17}Al_{12}$ at grain boundary, massive primary phase Mg_2Si and Chinese script eutectic Mg_2Si(a coarse dendritic morphology).

When adding 0.2wt. %Sr(Fig. 1(b)), the eutectic Mg_2Si phase changed from Chinese script to irregular blocky, while Sr content reached 0.4 %(wt. pct), Chinese characters were almost disappeared, the matrix was filled with bulk phase and the island of particles. The morphology of the Chinese script Mg_2Si phase morphology had been refined but to an irregular shape. The addition of 1% Sr, the microstructure emerged a large number of needle-shape phase and particulate dispersed phase.

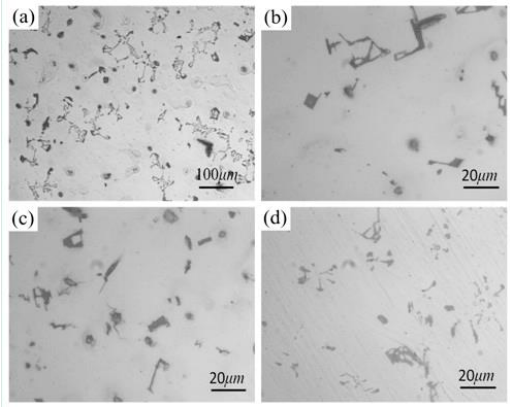

Fig. 1. As-cast microstructure of AS31 alloys and those with Sr addition: (a) 0 (b) 0.2 (c) 0.4 (d) 1.

Fig. 2 shows the resulting SEM images of experimental alloys. It was found from SEM Fig. 2(a) that the Mg_2Si phases in the AS31 alloy unmodified exhibited coarse Chinese script morphology. However, after adding 0.2 wt. %, 0.4 wt. %Sr and 1.0 wt. %Sr to AS31 alloy, the Chinese script Mg_2Si phases were modified and refined obviously. The Mg_2Si phase changed from coarse Chinese shape to fine granule and irregular polygonal shapes, this result was consistent with previous researches [15-17]. Furthermore, the average size of primary Mg_2Si (as shown in Fig. 3) decreased from about 36 μm to 17 μm.

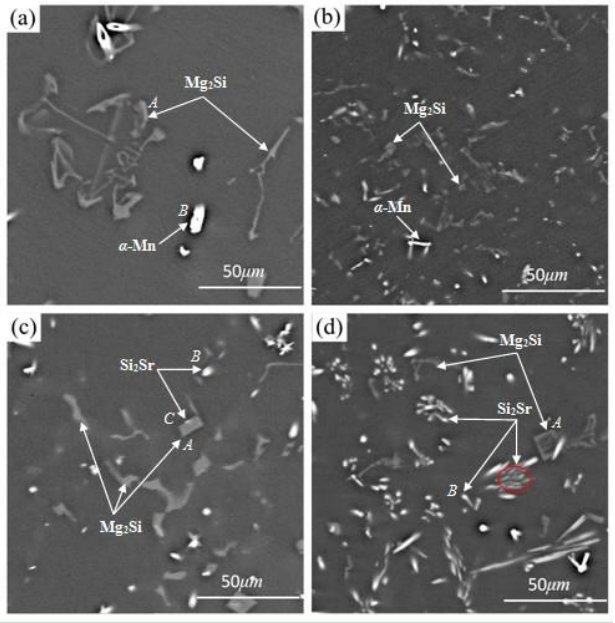

Fig. 2. SEM (BSE) images of AS31 alloys without and with Sr addition: (a) 0 (b) 0.2 (c) 0.4 (d) 1.

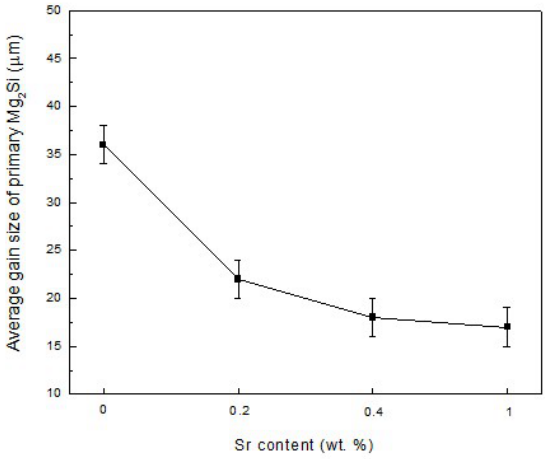

Fig. 3. The grain size of as-cast samples containing different levels of Sr.

Fig. 4 shows the X-ray mapping results of the Fig. 2(a), the highlight area in the presence of rich-Mn compounds, through the EDS analysis of the average concentration: Mn: 55.41, Mg: 30.14, Al: 12.81, Si: 1.64(wt. %) (Six points average results), M. Celikin et al [18] believed that the polygon precipitated was primary α-Mn phase, the primary α-Mn particles that existed in the intradendritic regions of the as-cast structure.

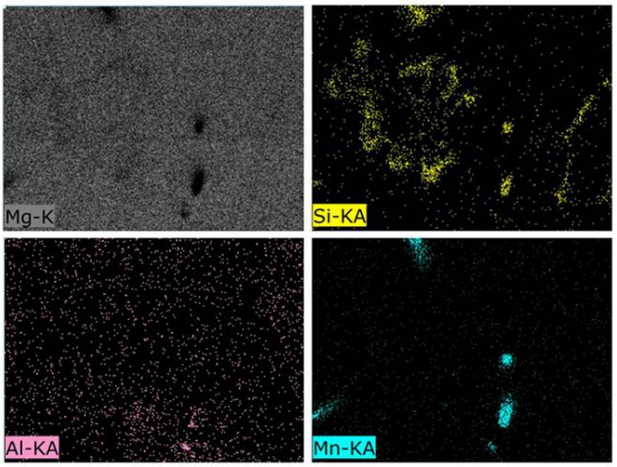

Fig. 4. X-ray mapping results for the as-cast AS31 alloy (Fig.2 (a)) without Sr addition.

As shown in Fig. 2 (b)-(d), the granular bright spot are observed in the SEM diagrams, which combining EDS analysis (Table 2) with the Si-Sr binary phase diagram (as Fig. 6 shown, data from TDnucl by FactSage) shows that it is likely to be Si_2Sr phase. In Fig. 2 (c) at point B, for example, by calculating the phase diagram corresponding to the X-axis value of the molar ratio (where the relative quality and the relative atomic mass of Sr, Si is: 20.84, 14.05 and 87.62, 28.09, respectively) was about 0.3223, which corresponds to the Si_2Sr phase of the Si-Sr phase diagram.

Table 2. EDS results of studied alloys (atomic fraction, %).

Position	Mg	Al	Si	Sr	Mn	Total/%
Fig.2(a)-*A*	69.68	3.32	27.30	-	-	100
Fig.2(a)-*B*	30.51	11.07	4.24	-	54.17	100
Fig.2(c)-*A*	67.33	-	32.67	-	-	100
Fig.2(c)-*B*	78.40	-	14.64	6.96	-	100
Fig.2(d)-*A*	91.44	0.48	8.08	-	-	100
Fig.2(d)-*B*	77.40	1.83	14.37	6.41	-	100

By the XRD diffraction analysis, as shown in the Fig. 4, α-Mg, $Mg_{17}Al_{12}$ and Mg_2Si were detected, and then the new phase Si_2Sr was discovered with 1% Sr addition.

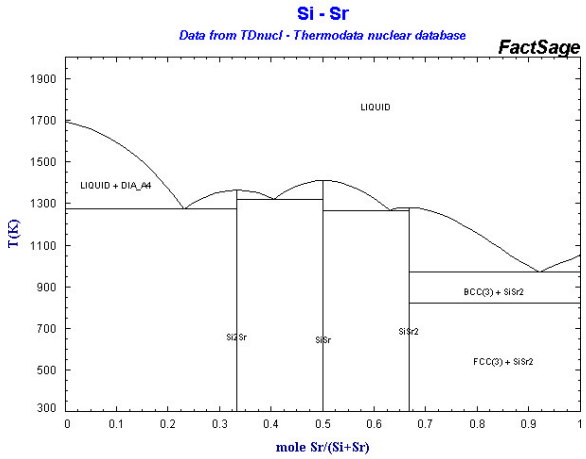

Fig. 5. Si-Sr binary phase diagram.

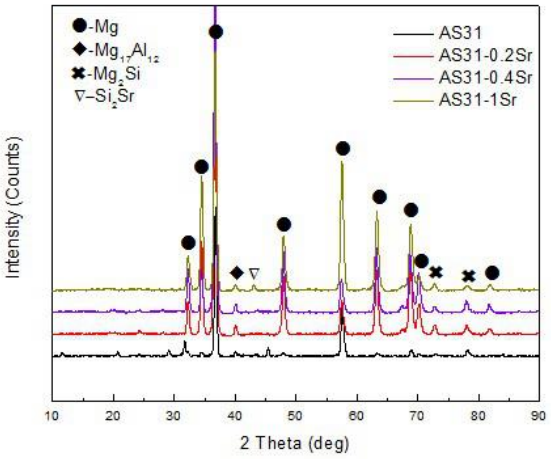

Fig. 6. XRD patterns for AS31 alloys with and without Sr addition.

4. Discussion

The effect of Sr refinement of the second phase in AS31 alloy is very obvious, especially, primary Mg_2Si and Chinese script eutectic Mg_2Si phase, and it is worth mentioning that, the number of Chinese script phase is significantly decreased with the increase of Sr content. When the Sr content reached 1%, the grain size tends to be stable. Sr Modification on the cast alloy hardness effect was so small that can be neglected. Through previous studies [19-21], if the Al content was higher, the alloy was easy to produce Al_4Sr, unlike these findings, because the Sr/Al ratio of the alloy AS31 was relatively low, it was unable to detect the presence of Al_4Sr at this experiment.

Through the observation of XRD diffraction curve, the diffraction peak of as-cast AS31 after Sr modification migrated to the large angle direction slightly, this change could be attributed to the interference effect of Sr

modification on the alloy internal components: Sr itself had a surface refinement effect, reducing the original phase grain size greatly; on the other hand, Sr could form new phase with other components of the alloy, and lead to the α-Mg diffraction peak angle narrowing.

Generally, if the third component could be roughly equal in both the distribution of the solid phase, it would result in the form of two phases state of instability, which found that cellular or even dendritic eutectic. The formation of dendritic crystal began with unstable planar interface rupture. If growth conditions were met dendritic crystal formation conditions will quickly become dendritic cell-like, thus showing a secondary dendrite arm. With the growth of the dendrite tip region, it discharged heat and soluted at the same time. With the increase of Sr content, Mg diffraction peaks showed significant improvement, theoretically, Sr replaced Mg with Si combined, according to the Bragg's law, because the Sr atomic radius (2.45 Å) is larger than the Mg atomic radius (1.72 Å), it may lead to the lattice expansion. From the XRD patterns, slight Mg_2Si diffraction peaks decrease could be seen. Considering the factors of the structural stability, Sr atoms were unlikely to replace Mg completely.

Through experiments and theoretical analysis of the data, the impact of Sr on the alloy could be considered the combination of two aspects: on the one hand, As the solubility of Sr in α-Mg was low (about 0.11 pct [22]), with the increase of Sr content, the excess Sr attached to the Mg_2Si peripheral, forcing primary Mg_2Si balling and suppressing dendritic structure and/ or twice dendrites orientation of dendrite Mg_2Si Chinese script phase. On the other hand Sr is likely to combine with the Si to produce Si_2Sr (the last needle phase).

The grain refinement effect of Sr to magnesium alloy could be considered to be inhibitory refinement effect of surface solid solution, its evolution process was shown in Fig. 7, in the unmodified AS31 alloy, coarse Chinese scripts were very obvious, with some massive primary Mg_2Si phase. When adding amount of Sr, the second phase was refined, and the refining effect was mainly reflected in the solution inhibited the growth of dendrite tip. ZHOU et al [23] suggested that dissociative Sr depress Mg_2Si growth manner, therefore, as the Sr content increased the Chinese script phase disintegrated gradually, when the dissociative Sr content reached a certain number (1 wt. % for this paper), some combined with Si element in Mg_2Si phase to generate acicular Si_2Sr phase. By EDS analysis, the intermediate region of needle-phase contains a large amount Si, Sr was relatively enriched in the edge of the needle-like phase, in a sense from the point of view that Si_2Sr was not a stable phase, but rather precipitates remnants of intermediate alloy phase. It was more likely formed as Sr modification effects on the Mg_2Si phase. The original Chinese script dendritic phase transited to needle-phase or thin strips phase as the center of block or irregular granular phase, and the original block or island phase due to the attachment or embedded of element Sr, while showing significant size refinement(from 36 μm to 17 μm).

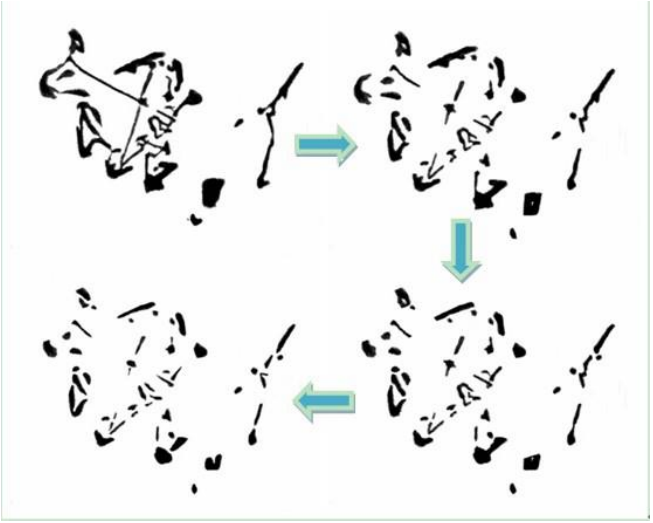

Fig. 7. The evolution process of Mg_2Si phase emoticons.

5. Conclusions

1) AS-cast AS31 magnesium alloy mainly consisted of the matrix α-Mg; divorced eutectic β-$Mg_{17}Al_{12}$ at grain boundary, massive primary phase Mg_2Si and Chinese script eutectic Mg_2Si. After adding 0.2 wt. %, 0.4 wt. %Sr and 1.0 wt. %Sr to AS31 alloy, the Chinese script Mg_2Si phases were modified and refined obviously. The Mg_2Si phase changed from coarse Chinese shape to fine granule and irregular polygonal shapes.

2) Sr could attach to the Mg_2Si peripheral, forcing primary Mg_2Si balling and suppressing dendritic structure and/ or twice dendrites orientation of dendrite Mg_2Si Chinese script phase. Sr was likely to combine with the Si to produce acicular Si_2Sr phase.

Acknowledgements

This work is supported by the Nature Science Foundation of Shandong Province, China. (No. ZR2010EQ021) and Science and Technology Development Plan Project of Shandong Province, China (No. 2011GGX10210).

References

[1] A. Luo, M. O. Pekguleryuz: J. Mater. Sci., **29**, 5259 (1994).
[2] E. Aghion, B. Bronfín, F. Von Buch, S. Schumann, H. Friedrich: JOM., **55**, 30 (2003).
[3] A. Modrea, S. Vlase, H. Teodorescu-Draghicescu, M. Mihalcica, M. R. Calin, C. Astalos, Optoelectron.

Adv. Mater. -Rapid Comm. **7**, 452 (2013).
[4] T. Sakai, J. -I. Koyama, Optoelectron. Adv. Mater. -Rapid Comm. **4**, 982 (2010).
[5] M. K. Kulekci: Int. J Adv. Manuf. Technol., **39**, 851 (2008).
[6] M. S. Dargusch, G. L. Dunlop, A. L. Bowles, K. Pettersen, P. Bakke, Metall. Mater. Trans. A., **35**, 1905 (2004).
[7] E. Evangelista, E. Gariboldi, O. Lohne, S. Spigarelli: Mater. Sic. Eng. A, **387**, 41 (2004).
[8] A. A. AL-Ghamdi, Omar A. AL-Hartomy, M. Cavas, Farid EL-Tantawy, F. Yakuphanoglu, Optoelectron. Adv. Mater. -Rapid Comm. **6**, 292 (2012).
[9] Y. Z. Lu, Q. D. Wang, X. Q. Zeng, W. J. Ding, Y. P. Zhu, J. Mater. Sci. Lett. **20**, 397 (2001).
[10] S. F. Liu, B. Li, X. H. Wang, W. Su, H. Han: J. Mater. Process. Technol., **209**, 3999 (2009).
[11] D. H. StJohn, M Qian, M. A. Easton, P. Cao, Z. Hildebrand: Metall. Mater. Trans. A, **36**, 1669 (2005).
[12] D. H. Song, C. W. Lee, K. Y. Nam, S. W. Lee, Y. H. Park, K. M. Cho, I. M. Park: Mater. Sci. Forum, **539**, 1784 (2007).
[13] G. Vitel, A. L. Paraschiv, M. G. Suru, N. Cimpoesu, L. G. Bujoreanu, Optoelectron. Adv. Mater. -Rapid Comm, **6**, 339 (2012).
[14] A. Sadeghi, M. Pekguleryuz: Mater. Charact., **62**, 742 (2011).
[15] M. B. Yang, F. S. Pan, J. Shen, L. Bai: Trans. Nonferrous Met. Soc. China, **19**, 287 (2009).
[16] H. Y. Wang, M. Zha, B. Liu, D. M. Wang, Q. C. Jiang: J. Alloys Compd., **480**, L25 (2009).
[17] M. Masoumi, M. Pekguleryuz: Mater. Sci. Eng. A, **529**, 207 (2011).
[18] M. Celikin, A. A. Kaya, M. Pekguleryuz: Mater. Sci. Eng. A, **550**, 39 (2012).
[19] A. T. Tang, F. S. Pan, M. B. Yang, R. J. Cheng: Mater. Trans., **6**, 1203 (2008).
[20] Y. Yang, X. D. Peng, H. M. Wen, B. L. Zheng, Y. Z. Zhou, W. D. Xie, E. J. Lavernia: Metall. Mater. Trans. A, **44**, 1101 (2013).
[21] T. Sato, M. V. Kral, Mater. Sci. Eng. A, **498**, 369 (2008).
[22] A. Suzuki, N. D. Sassock, L. Riester, E. Lara-Curzio, J. W. Jones, T. M. Pollock, Metall. Mater. Trans. A, **38**, 420 (2007).
[23] J. X. Zhou, Y. S. Yang, S. Q. Tang, C. W. Tian, Mater. Sci. Forum, **686**, 125 (2011).

*Corresponding author: wx1979875@hotmail.com